GMR Genetics and Molecular Research
Online Journal
ISSN:1676-5680

CpG ODN 1826 enhances radiosensitivity of the human lung cancer cell line A549 in a rat model

W. Yan, T.-Y. Sun, C.-M. Yang, M. Jia, J. Li, H.-L. Tang and Y.-F. Zhou

The Cadre Ward of Air Force General Hospital, Beijing, China

Corresponding author: T.-Y. Sun
E-mail: suntiye_sty@163.com

Genet. Mol. Res. 14 (3): 9804-9812 (2015)
Received January 31, 2015
Accepted May 11, 2015
Published August 19, 2015
DOI http://dx.doi.org/10.4238/2015.August.19.13

ABSTRACT. This study investigated the effects of CpG ODN1826 plus radiotherapy (RT) on tumor growth and angiogenesis of subcutaneous tumor in a rat model. Four treatment groups were tested in which rats were injected with 100 µL CpG ODN1826 (1 µg/µL) or 100 µL vehicle, with and without exposure to 8 Gy after 2 h. At 7 days after inoculation of lung cancer cells, drugs were injected in the tumor and radiation was administered over 5 days, after which the rate of tumor inhibition was calculated. Expression of VEGF-C in tumor tissue was seen in 10, 50, 80, and 100% of tumors in the CpG ODN1826 + RT, CpG ODN1826, vehicle + RT, and vehicle alone groups, respectively, while positive expression of NRP-1 was seen in 10, 40, 90, and 100% of tumors. The decreases in expression of VEGF-C mRNA in the CpG ODN1826 + RT and CpG ODN1826 groups compared with the NS + RT and NS groups were significant ($P < 0.01$), as were the decreases in NRP-1 mRNA in the CpG ODN1826 + RT group compared with the CpG ODN1826 group ($P < 0.01$). Thus, CpG ODN1826 can significantly inhibit tumor growth in a rat model, the mechanism of which may be

related to inhibition of the expression of VEGF-C and NRP-1, which have an inhibitory effect on angiogenesis.

Key words: CpG ODN; Vascular endothelial growth factor-C; Neuropilin-1; Immunohistochemical staining

INTRODUCTION

Radiotherapy (RT) is an important treatment modality for patients with advanced cancer. Since invasive growth, metastasis, and prognosis of lung cancer depends on growth of blood vessels, blocking or inhibiting angiogenesis can inhibit the growth and metastasis of tumor cells. Vascular endothelial growth factor (VEGF), as a vascular growth factor, acts specifically on vascular endothelial cells, which are closely related to both tumor growth and metastasis (Cross and Claesson-Welsh, 2001). Previous studies have shown that CpG ODN1826 (10 μg/mL) together with beta irradiation can considerably increase the radiosensitivity of the human pulmonary adenocarcinoma cell line A549 (Yan et al., 2011). The present study established a rat subcutaneous tumor model, based on early stage experiments *in vitro*, with the aim of investigating the effects of CpG ODN1826 on tumor growth and elucidating the underlying mechanisms of anti-angiogenesis caused by CpG ODN1826.

MATERIAL AND METHODS

Materials

Human pulmonary adenocarcinoma cell line A549 cells were kindly provided by the Respiratory Disease Research Institute of Xinqiao Hospital, Third Military Medical University.

A total of 40 rats (20 males, 20 females) were purchased from the Experimental Animal Center of the Third Military Medical University, and they were housed in a sterile laminar flow chamber.

DMEM, fetal bovine serum, and MTT were purchased, respectively, from Gibco (BRL, Rockville, MD, USA), PAA Company (Changzhou, China), and Amerisu Company (S Plainfield, NJ, USA). LPS and DMSO were purchased from Sigma (Berlin, Germany). CpG ODN1826, comprising a nucleotide sequence of 5'-TCCATGACGTTCCTGACGTT-3' with whole skeleton glucosinolates, was synthesized by using Takara (Osaka, Japan). After centrifugation, CpG ODN1826 was brought to a concentration of 10 μg/μL by the addition of ultrapure water. DAB (3,3'-diaminobenzidine) chromogenic reagent was purchased from Boster Company in Wuhan (China). MMLV reverse transcriptase kits (Gibco) were purchased from Jingmei Biotechnology Company, Ltd.

Methods

Establishment of an animal model

A549 cells were digested with 0.25% trypsin and then diluted into a single cell suspension with fresh DMEM medium. Cells were then centrifuged, washed twice with ice-cold normal saline, and brought to a concentration of 2 x 10^7 cells/mL; 0.15 mL cell suspension (4 x

10^6 cells) was inoculated into the subcutis of the back of nude rats using a 1-mL syringe. Animals were then housed in a sterile laminar flow chamber and changes in tumor growth were observed. After tumors had grown to 1 cm (within 1 week), the rats were divided into groups and experiments were performed.

Animal groups and administration of study drugs

Nude rats were randomly divided into four groups, each composed of 10 rats. All rats were injected with tumor cells at the same time. The four treatment groups were as follows: 100 µL 1 µg/µL CpG ODN1826; 100 µL 1 µg/µL CpG ODN1826 + RT, followed by exposure after 2 h to 8 Gy; NS + RT, injected with 100 µL physiological saline injection and exposed after 2 h to 8 Gy; NS, injected with 100 µL physiological saline injection.

Irradiation conditions and methods

Rats were given an intraperitoneal injection of 1% pentobarbital at a dose of 0.004 mL/g to induce coma as determined by stable breathing and heartbeat after 5 min. Next, rats were placed in a special sterile box with dual air filters. The tumor site was placed in the central beam apart from the edge beam more than 1 cm and the remainder of the body was outside the radiation field. The experiment used a linear accelerator with a radiation dose of 6 mV beta particles. Animals in each group were exposed at the same time once every 3 days with an irradiation dose of 400 cGy per minute. After 2 h, the tumor-burdened rats were round.

Five days after RT, the rats were decapitated; tumor tissue was removed, and fixed by immersing in 10% formaldehyde solution. Specimens were dehydrated and embedded with paraffin; 4-µm tissue slices were used for analysis.

Observational index

The width (*a*), length (*b*), and height (*c*) of tumors were measured using a caliper, and the approximate volume (*V*) was calculated using the following formula: V = n / 6 (abc). Units were expressed in mL.

The observational index is the tumor inhibition rate: the inhibitory rate (%) was equal to the ratio between the treatment and control groups considering the difference in the average volume of tumor at the beginning and end of the experiment.

Immunohistochemical analysis

According to the previous protocol (Sun et al., 2007), gastric cancer tissue samples were fixed in 10% neutral formaldehyde, embedded in paraffin. For immunohistochemical analysis, 5-µm sections were used. Sections were attached to the slide and air dried before heating at 60°C in an oven for 2 h. After dewaxing with dimethylbenzene, tissues were hydrated using a graded series of ethanol. A solution of methanol and hydrogen peroxide (3 mL/L) was used to inhibit endogenous peroxidase and further retrieved the antigen. Tissue sections were heated for 10 min in citrate buffer (pH 6.0), followed by incubation in normal sheep serum, after which neuropilin-1 (NRP-1) (dilution 1:50) or VEGF-C (dilution 1:25) was added and incubated at 7°C for 30 min. Slides were then incubated with 5% serum for 30 min at

room temperature to block nonspecific binding sites. The next day, tissues were washed with PBS 3 times for 5 min each, and slices were then incubated successively with the first antibody (NRP-1 antibodies diluted 1:75), the second antibody (biotin labeled IgG diluted 1:400), and streptomycin avidin labeled with horseradish peroxidase (diluted 1:400) for 30 min. The chromogen DAB was then added after rinsing with PBS until a wood grain pattern was obtained. The slice was finally mounted with neutral resin and observed under a light microscope. PBS was used instead of the first antibody as a negative control.

Scoring of immunohistochemistry

Positive cells appeared as tan or brown granules in the cell membrane or cytoplasm, respectively, with a clear line but no obvious background color. Five high power fields of each section (400X) were examined to classify immunohistochemical results according to the percentage of positive cells as follows: negative (-), <5% positive cells; weakly positive (+), 5-24% positive cells; moderately positive (++), 25-49% positive cells; strongly positive (+++), >50% positive cells.

Detection of VEGF-C mRNA in lung cancer tissues by using RT-PCR

Lung cancer tissue samples were frozen in liquid nitrogen, and a mortar was used to grind the tissues in a powder under liquid nitrogen. Total RNA was extracted using a kit (Bioteck, Beijing, China) according to the manufacturer's instructions and quantified using a spectrophotometer. Two grams of RNA was used to synthesize cDNA using a MMLV reverse transcriptase kit. The cDNA obtained was used as a template for PCR to amplify VEGF-C. β-actin was used as an internal reference using the following primers: 5'-GTGGGGC-GCCCCAGGCACC
A-3' and 5'-CTTCCTTAATGTCACGCACGATTTC-3'. The length of the amplified fragment was 480 bp. VEGF-C was amplified using the following primers: 5'-AATGTGGGGCCAACC GAGAA-3' and 5'-CCAATATGAAGGGACACAACG-3'. The amplified fragment was 285 bp in length. PCR conditions were as follows: denatured at 94°C for 2 min, followed by 30 cycles of 94°C for 30 s, 65°C for 30 s and 72°C for 30 s, followed by a final extension step at 72°C for 10 min. All PCR products were electrophoresed on a 1.5% agarose gel containing ethidium bromide. A gel image analysis system was used to convert the image to gray scale and determine the relative content of VEGF-C mRNA, which was normalized to β-actin.

Detection of NRP-1 mRNA in lung cancer tissues by using RT-PCR

PCR for NRP-1 mRNA was carried out as described above. β-actin was used as an internal standard. The upstream primer used to amplify NRP-1 was 5'-GTGGTCGTGCTGG TCCTC-3' and the downstream primer was 5'-CTCTGGCAACATGGCTTTCG-3'. The amplified fragment was 210 bp in length. The RT-PCR results of VEGF-C and NRP-1 were analyzed using the quantitative analysis software Gel-PRO Analyzer to calculate the integral optical density (IOD). The ratio of the target gene's IOD and that of beta-actin, or the IOD value standardization (normalized integrated intensity, NII) was used to calculate the NII x 100% and used to compare the results of RT-PCR.

Statistical methods

Statistical analyses were performed using the SPSS version 13.0 software (SPSS, Inc., Chicago, IL, USA). All measurements are reported as means and standard deviations. All experiments were repeated at least three times. Numerical data was compared by using a two-sample *t*-test, while measurements were compared with reported Fisher exact test. A $P < 0.05$ was considered to be statistically significant.

RESULTS

Tumor implantation and pathological examination

After implantation of A549 cells under the skin of the back, nude rats showed tumor formation in 6 to 7 days. The success rate of implantation was 100%, with tumor sizes of 20-60 mm. Implanted tumors were visible on the back as irregular, single, spherical masses under the skin that were non-adherent to underlying layers. General conditions of the animals gradually decreased with time as the tumor volume increased. Visible tumors showed hematoma on the third day in the groups that received irradiation. After 14 days, tumor volume in the CpG ODN1826 and CpG ODN1826 + RT groups was visibly reduced compared with control groups. Macroscopically, few blood vessels were visible in the tumors and tumor collapse was evident in the CpG ODN1826 + RT group. In the control group, blood capillary density of tumors increased with vasodilation. However, tumors in the CpG ODN1826 group contained only a small amount of visible blood capillaries.

Pathological examination showed that subcutaneous tumor tissue had characteristics that were similar to the human pulmonary adenocarcinoma cell line A549. Implanted tumor tissues showed extensive areas of partial necrosis along with the presence of hyperchromatic magnocellular nuclei when stained with hematoxylin and eosin.

Tumor growth

Subcutaneous tumor implantation was successful in all animals. At 7 days after implantation, there was no significant difference in tumor size between animals. At 7 days after irradiation, all animals were in good overall conditions, with no deaths, and regular eating and drinking habits. Tumor growth in all four groups was similar until about day 7, after which growth was clearly slower in the CpG ODN1826 group. Growth was highest in the group that received saline without radiation. Overall, the growth trend was as follows, in order of highest to lowest: NS, NS + RT, CpG ODN1826, and CpG ODN1826 + RT. The differences between groups were significant ($P < 0.01$). Changes in tumor growth are shown in Figure 1.

Inhibitory effects of CpG ODN1826 on tumor growth

After 7 days, in the CpG ODN1826 + RT group there was visible reduction of tumor volume compared with the control groups ($P < 0.01$). At 14 days after irradiation, shrinkage of tumor was not observed in the CpG ODN1826 + RT group. The rate of inhibition of tumor growth in the irradiation groups was at least 66.7 ± 0.27%, and 21.5 ± 0.15% in the CpG

ODN1826 group, compared to 15.1 ± 0.89% in the control group. The differences between groups were statistically significant ($P < 0.01$) as seen in Figure 2.

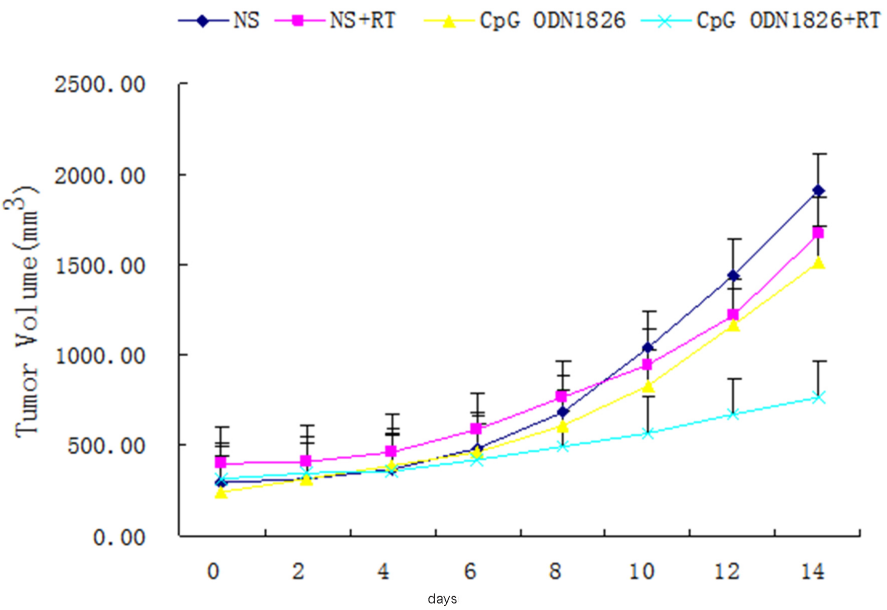

Figure 1. Effects of CpG ODN1826 on tumor growth in a rat model (N = 40).

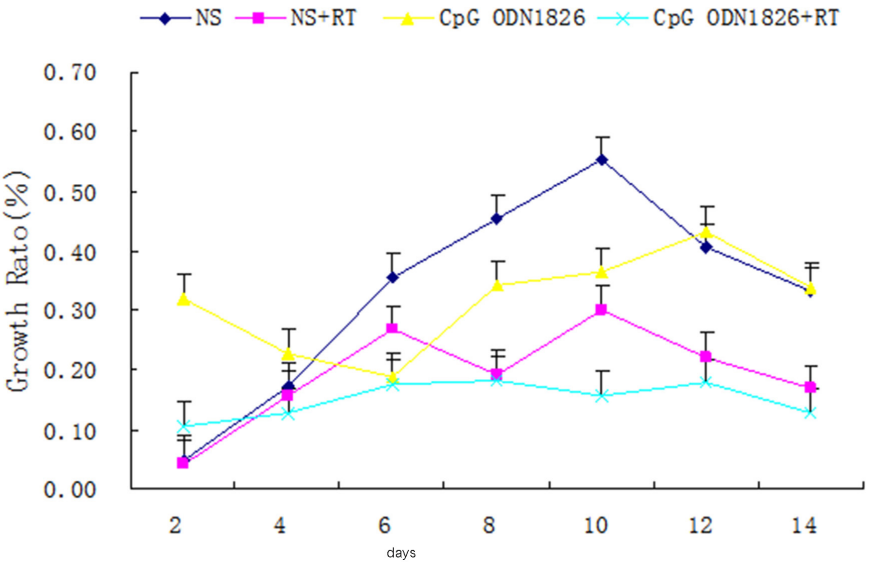

Figure 2. Inhibitory effects of CpG ODN1826 on tumor growth in a rat model (N = 40).

Expression of VEGF-C and NRP-1 in tumor tissues

Expression of VEGF-C and NRP-1 was detected mainly in the cytoplasm of tumor cells. Positive expression was observed as focal or diffuse distribution, with no nuclear staining. In the NS group, expression of VEGF-C and NRP-1 was seen in all 10 animals (100%), compared with 80 and 90%, respectively, in the NS + RT group. Expression of VEGF-C and NRP-1 was seen in 50 and 40% of animals in the CpG ODN1826 group, respectively. Lastly, in the CpG ODN1826 + RT group positive staining of VEGF-C and NRP-1 was seen in only 1 animal (10%) (Table 1). The differences between groups were significant ($P < 0.01$).

Table 1. Expression of VEGF-C and NRP-1 in tumor tissues.

Group	N	VEGF-C		%	NRP-1		%
		Negative (N)	Positive (N)		Negative (N)	Positive (N)	
CpG ODN + RT	10	9	1	10[a]	9	1	10[a]
CpG ODN	10	5	5	50[a]	6	4	40[a]
NS + RT	10	2	8	80[a]	1	9	90[a]
NS	10	0	10	100	0	10	100

VEGF-C = vascular endothelial growth factor-C; NRP-1 = neuropilin-1; NS = physiological saline; RT = radiotherapy.

Effects of CpG ODN1826 on VEGF-C and NRP-1 mRNAs as detected by using RT-PCR

Levels of VEGF-C and NRP-1 mRNAs in the tumor tissue of each group were detected by using RT-PCR and normalized to the levels of beta-actin (Figure 3). Expression of both VEGF-C and NRP-1 mRNAs in the CpG ODN1826 + RT group was significantly decreased compared with the other three groups ($P < 0.01$). Thus, CpG ODN1826 has a significant inhibitory effect on the expression of VEGF-C and NRP-1 mRNAs.

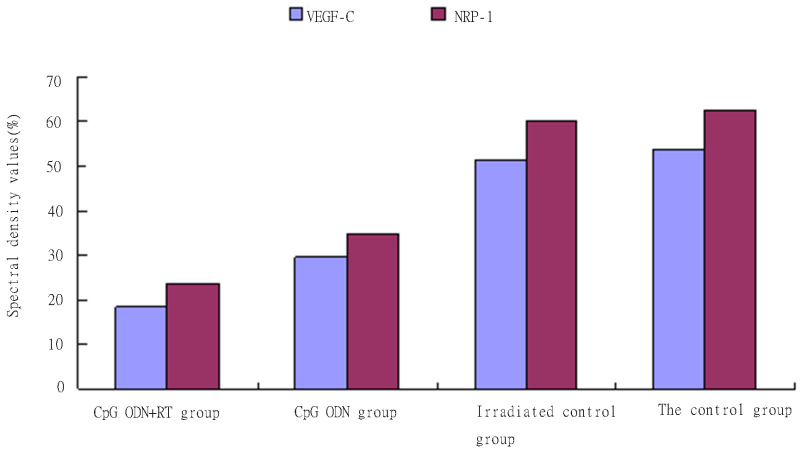

Figure 3. Effects of CpG ODN1826 on VEGF-C and NRP-1 mRNAs as detected by using RT-PCR. VEGF-C, vascular endothelial growth factor-C; NRP-1, neuropilin-1, RT-PCR, reverse transcription polymerase chain reaction.

DISCUSSION

Angiogenesis is an important process for infiltrating growth and tumor metastasis since growth of solid tumors requires formation of new blood vessels. A number of studies have confirmed that adhesion and migration of vascular endothelial cells to the tumor is an important step in tumor angiogenesis. In this regard, MMP-c, VEGF, and other substances promote angiogenesis and can cause the migration of endothelial cells, which accelerate tumor angiogenesis and metastasis. VEGF, as a major regulatory factor of angiogenesis, has been a primary focus of cancer research. The VEGF family includes VEGF-A, VEGF-B, VEGF-C, VEGF-D, VEGF-E, and placental growth factor, along with receptors of VEGF including VEGFR-1 (Fit1), VEGFR-2 (FLK1/KDR), and VEGFR-3 (Fit4). Recently, NRP-1 and NRP-2 have been discovered to be novel VEGF receptors, and are expressed in both tumor cells and endothelial cells. The VEGF family of proteins can not only selectively enhance endothelial cell mitosis in blood and lymphatic vessels, but also stimulate proliferation of endothelial cells to promote blood vessel formation. In such a situation, the permeability of blood vessels and capillaries is increased and a new capillary network is promoted. Finally, these molecules promote tumor growth, play an important role in angiogenesis, and may be a marker of tumor progression (Stephenson et al., 2002; Murga et al., 2005). Akagi et al. (2003) detected 7 kinds of protein expression of NRP-1 mRNA and EGF-R in gastric cancer cells in humans. In particular, it was suggested that the regulation of expression of NRP-1 in gastric cancer is closely related to the EGF-EGFR system, and that activation of EGF-R may be involved in regulation of expression on VEGF and NRP-1 through multiple signaling pathways. In addition, activation of EGF-R also promoted the formation of blood vessels in gastric cancer. Miao et al. (2000) used the rat prostate cancer cell line AT2.1 to overexpress NRP-1. It was seen that overexpression of the NRP-1 gene can promote tumor growth and proliferation by enhancing tumor angiogenesis. Kawakami et al. (2002) studied the expression of NRP-1 and NRP-2 in non-small cell lung cancer and found that both enhanced vascularization and promoted tumor progression.

Herein, CpG ODN1826 alone and in combination with RT was found to have an inhibitory effect on tumor angiogenesis and growth of subcutaneous tumor in a rat model. Moreover, blood vessels around the tumor were relatively sparse in the CpG ODN1826 treatment groups compared with the NS and NS + RT groups ($P < 0.01$). At the same time, immunohistochemical analysis showed that the rate of positive expression of VEGF-C and NRP-1 was low in both the CpG ODN1826 treatment groups. Similarly, RT-PCR confirmed that expression of both VEGF-C and NRP-1 mRNAs was significantly reduced in both the CpG ODN1826 treatment groups. Furthermore, the inhibitory effects of CpG ODN1826 + RT on the expression of VEGF-C mRNA and NRP-1 mRNA indicate that both CpG ODN1826 + RT and CpG ODN1826 can effectively inhibit the formation of blood vessels surrounding A549 cells in tumor tissues, which are essential for tumor growth. In fact, significant inhibition of tumor growth was also seen in the CpG ODN1826 groups. CpG ODN1826 had synergistic effect on suppressing tumor growth when combined with radiation. We speculate that CpG ODN1826 may enhance the irradiation effects of beta rays, not only by inhibiting the expression of VEGF-C and NRP-1, but also by inhibiting the synergistic expression of NRP-1 and VEGFR. Decreased in the binding of VEGF and VEGFR is thus likely to control or block the amplification of VEGF signaling. This synergistic effect effectively reduces the formation of new blood vessels around tumor tissue, eventually inhibiting the growth of tumor by killing endothelial cells (Bernatchez et al., 2002). The results seen herein affirm that one of the main

mechanisms of CpG ODN1826 inhibition of subcutaneous tumor growth and angiogenesis in rat lung cancer is through modulation of expression of VEGF-C and NRP-1. Although our results show that treatment of lung cancer with CpG ODN1826 in association with radiation has good experimental efficacy, the relationship between CpG ODN1826 in combination with beta radiation and the molecules involved in the signaling pathways such as NRP-1, VEGF-C, and VEGFR merit further in-depth study.

REFERENCES

Akagi M, Kawaguchi M, Lju W, McCarty MF, et al. (2003). Induction of neuropilin-1 and vascular endothelial growth factor by epidermal growth factor in human gastric cancer cell. *Br. J. Cancer* 88: 796-802.

Bernatchez PN, Rollin S, Soker S and Sirois MG (2002). Relative effects of VEGF-A and VEGF-C on endothelial cell proliferation, migration and PAF synthesis: Role of neuropilin-1. *J. Cell Biochem.* 85: 629-639.

Cross MJ and Claesson-Welsh L (2001). FGF and VEGF function in angiogenesis: signalling pathways, biological responses and therapeutic inhibition. *Trends Pharmacol. Sci.* 22: 201-207.

Kawakami T, Tokunaga T, Hatanaka H, Kijima H, et al. (2002). Neuropilin 1 and neuropilin 2 co-expression is significantly correlated with increased vascularity and poor prognosis in non-small cell lung carcinoma. *Cancer* 95: 2196-2201.

Miao HQ, Lee P, Lin H, Soker S, et al. (2000). Neuropilin-1 expression by tumor cells promotes tumor angiogenesis and progression. *FASEB J.* 14: 2532-2539.

Murga M, Fernandez-Capetillo O and Tosato G (2005). Neuropilin-1 regulates attachment in human endothelial cells independently of vascular endothelial growth factor receptor-2. *Blood* 105: 1992-1999.

Stephenson JM, Banerjee S, Saxena NK, Cherian R, et al. (2002). Neuropilin-1 is differentially expressed in myoepithelial cells and vascular smooth muscle cells in preneoplastic and neoplastic human breast: a possible marker for the progression of breast cancer. *Int. J. Cancer* 101: 409-414.

Sun TY, Zhao YL, Yan W, Shi Y, et al. (2007). CXCR4 and VEGF-C expression and its relationship with lymph node metastasis in gastric carcinoma. *Xi Nan Guo Fang Yi Yao* 17: 285-288.

Yan W, Sun TY, Yang CM, Jia M, et al. (2011). The mechanism of CpG ODN enhancing the radiosensitivity of lung cancer cell line A549. *Zhong Hua Lin Chuang Yi Shi Za Zhi* 5: 3768-3772.

